Journal of Medicinal Chemistry

Article

Cyclopentadienyl-Ruthenium(II) and Iron(II) Organometallic Compounds with Carbohydrate Derivative Ligands as Good Colorectal Anticancer Agents.

Ana Cristina Fernandes, Pedro Florindo, Diane M Pereira, Pedro M. Borralho, Cecília M.P. Rodrigues, and Maria Fátima Minas da Piedade

J. Med. Chem., **Just Accepted Manuscript** • DOI: 10.1021/acs.jmedchem.5b00403 • Publication Date (Web): 29 Apr 2015

Cyclopentadienyl-Ruthenium(II) and Iron(II) Organometallic Compounds with Carbohydrate Derivative Ligands as Good Colorectal Anticancer Agents.

Pedro R. Florindo,[a] Diane M. Pereira,[b] Pedro M. Borralho,[b] Cecília M.P. Rodrigues,[b] Maria F.M. Piedade[a,c] and Ana C. Fernandes[a]*.*

[a] Centro de Química Estrutural, Instituto Superior Técnico, Universidade de Lisboa, Av. Rovisco Pais, 1049-001 Lisboa, Portugal.

[b] Research Institute for Medicines (iMed.ULisboa), Faculty of Pharmacy, Universidade de Lisboa, Av. Prof. Gama Pinto, 1649-003 Lisboa, Portugal.

[c]Departamento de Química e Bioquímica, Faculdade de Ciências da Universidade de Lisboa, Campo Grande, 1749-016 Lisboa, Portugal.

Ruthenium(II); Iron(II); Carbohydrates; Colon Anticancer Agents; Metallo-Drugs; Cytotoxicity.

ABSTRACT: New ruthenium(II) and iron(II) organometallic compounds of general formula $[(\eta^5\text{-}C_5H_5)M(PP)\mathbf{Lc}][PF_6]$, bearing carbohydrate derivative ligands (**Lc**) were prepared and fully characterized, and the crystal structures of five of those compounds

were determined by X-ray diffraction studies. Cell viability of colon cancer HCT116 cell line was determined for a total of twenty-three organometallic compounds and SAR's data analysis within this library showed an interesting dependency of the cytotoxic activity on the carbohydrate moiety, linker, phosphane co-ligands and metal center. More importantly, two compounds, **14Ru** and **18Ru**, matched oxaliplatin IC_{50} (0.45 μM), the standard metallo-drug used in CC chemotherapeutics, and our leading compound **14Ru** was shown to be significantly more cytotoxic than oxaliplatin to HCT116 cells, triggering higher levels of caspase-3 and -7 activity, and apoptosis in a dose-dependent manner.

1. Introduction

Since the discovery of cisplatin in 1965,[1] the quest for metal-based drugs has been driven by the hope that it might be replaced by a less-expensive metal complex, with fewer side effects and improved therapeutic value. Metal-based drugs are very attractive due to its great versatility in terms of coordination number, oxidation state and geometric orientation around the metal center, and to the metal itself. Among other metals studied for their anticancer properties, ruthenium compounds present special properties, such as capacity to mimic iron by binding to biological molecules, reduced general toxicity and strong affinity to cancer tissues over normal tissues, making them appealing candidates as anticancer drugs.[2] Two ruthenium(III) compounds, NAMI-A ([ImH][trans-Ru(III)Cl_4Im(Me_2SO)]; Im = imidazol)[3] and KP1019 ([Hind][trans-Ru(III)Cl_4(Ind)$_2$], Ind = indazol)[4] were featured in clinical trials as anti-metastatic and anticancer agents, respectively, but exposed problems concerning their delivery and associated side effects. Clinical studies have shown that NAMI-A application may cause skin blisters lasting up to several months and resulting in intense pain.[5] In turn,

KP1019 presents low solubility, which makes it challenging to obtain proper dosage in clinical trials.[6]

Organo-ruthenium(II) complexes seem suitable drug candidates. Ruthenium(II)-arene complexes, of general formula [(η^6-C_6H_6)Ru(L1)(L2)(L3)], constitute the most studied class of ruthenium compounds, exhibiting promising anticancer activity both *in vitro* and *in vivo*. The complexes are stable and their framework provides a considerable scope for design optimization, in terms of biological activity and of minimizing side-effects, through variations in the arene and in the other coordinated ligands.[2] Two compounds of this class, RM175 and RAPTA-T (Figure 1), entered pre-clinical development stages, due to its activity against primary and metastasis tumors, respectively. [2d]

Isoelectronic cyclopentadienyl-ruthenium(II) compounds [(η^5-C_5H_5)Ru(L1)(L2)(L3)][X] have been also subject to posterior research. Compounds of general formulas [Ru(η^5-C_5H_5)(PP)(L)][X] (PP= mono- or bidentate phosphanes; L= N-donor ligand; X= counter-ion) and [Ru(η^5-C_5H_5)(P)(N-N)][X] (P= phosphane ligand; N-N= bidentate ligand; X= counter-ion) showed significant toxicity against a variety of cancer cell lines, namely LoVo (human colon adenocarcinoma), MiaPaCa (pancreatic cancer), HL-60 (human leukemia), A2780 and A2780CisR (human ovarian, cisplatin-sensitive and cisplatin-resistant, respectively), MCF7 and MDAMB231 (human breast, estrogen dependent and independent, respectively), PC3 (human prostate) and HeLa (cervical carcinoma) cancer cell lines, with IC_{50} values consistently lower than cisplatin's, up to 200-fold in some cases.[7] Stausporine mimetic cyclopentadienyl-ruthenium compounds, exhibited affinity and selectivity for proto-oncogenic enzymes such as GSK3, Pim-1, PI3K.7a-d In particular, compound DW1/2 (Fig. 1) the most studied within this sub-class, inhibits either GSK3beta and PI3K in human melanoma

cells, leading to apoptotic cell death mediated by p53 and the mitochondrial pathway. Compound $[(\eta^5\text{-}C_5H_5)Ru(bipy)(PPh_3)]^+$, TM34, and derivatives, such as its water soluble analogue TM85 (Figure 1) were later studied for its anticancer properties, revealing highly cytotoxic against a large spectra of cancer cell lines. Similarly to DW1/2, TM34 revealed as a strong PARP-1 inhibitor, an enzyme involved in DNA repair mechanisms and apoptosis pathways,[7h] and TM85 was found to induce cell death involving the Golgi apparatus.[7k]

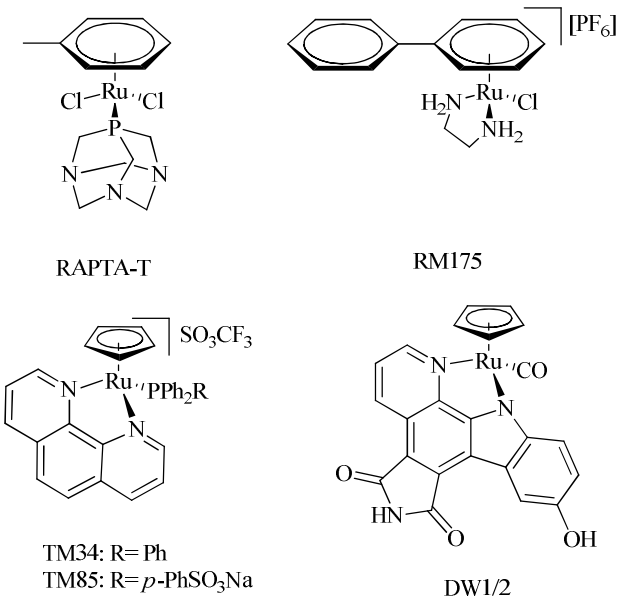

Figure 1. Most studied anticancer "half-sandwich" ruthenium(II) compounds.

What about iron, the bio-metal mimicked by ruthenium? Curiously enough, this metal has attracted much less interest regarding anticancer research. Ferrociffens, "sandwich" ferrocene derivatives of Tamoxifen, a drug used to treat breast cancer, revealed anticancer activity against estrogen-dependent (MCF7) and independent (MDA-MB231) breast cancer cell lines, while the parent drug is inactive in the hormone-independent cell line.[8] Other classes of ferrocene derivatives have been studied, also providing promising results.[9] Ferrocene derivatives suffer, however, from

bioavailability problems, restricting its clinical use.[10] More recently, "half-sandwich" cyclopentadienyl-iron(II) compounds of general formula [Ru(η^5-C_5H_5)(Dppe)(L)][CF_3SO_3] revealed good cytotoxic activities against A2780 (ovarian), MCF7 (breast), HeLa (cervical carcinoma),[11a] and HL-60 (human leukemia)[11b] cancer cell lines, with IC_{50} values up to 30 x lower than cisplatin. Similarly to ruthenium analogues, these early results envision this class of compounds as very promising to the development of anticancer metallo-drug candidates.

We have been focusing in developing anticancer organometallic compounds bearing bio-derivative ligands. Carbohydrates are the largest class of natural compounds, readily available and renewable, providing a large number of functional groups and several stereogenic centers *per* molecule, and each hydroxyl group offers the opportunity of selective modification and coordination, also granting some control over the lipophilicity/aqueous solubility of derivative complexes. Recently we reported the synthesis and characterization of cyclopentadienyl-ruthenium(II) complexes bearing carbohydrate (galactose and fructose) derivative ligands, which revealed outstanding cytotoxic activities against HeLa (cervical carcinoma) cancer cells, much better than cisplatin.[7m]

We now turn our attention to colon cancer (CC), a high profile cancer type, displaying both high incidence and associated mortality.[12] So far, synthetic chemical compounds such as 5-fluorouracil (5-FU) and oxaliplatin, a second-generation platinum chemotherapeutic drug used specifically for CC, are still the first choice of treatment for CC patients in advanced stages (Figure 2). Nonetheless, problems such as innate/acquired resistance, lack of selectivity for cancer tissues and severe associated side-effects, constitute major obstacles for this cornerstone chemotherapeutic agents.[13] Thus, the discovery of new agents with fewer side effects and improved therapeutic

value together with the clarification of the pathways by which they operate, is of great interest to the development of anticancer drug.

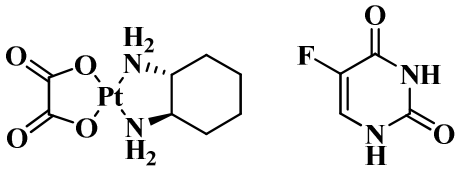

Oxaliplatin 5-Fluorouracil

Figure 2. Standard CC chemotherapeutic agents.

Here, we disclose the extension of our library of Group 8 anticancer organometallic compounds, with the development of new cyclopentadienyl-Ru(II) and Fe(II) compounds bearing D-ribose, D-xylose, D-galactose and D-glucose derivative ligands, obtained in one-pot synthesis from commercial raw sugars. The cytotoxicity of twenty organometallic compounds studied was evaluated in HCT116 CC cells, allowing the determination of Structure-Activity Relationships (SAR's), concerning the variation of metal centers, carbohydrate derivative ligands and phosphane co-ligands. *In vitro* studies of our leading compound, **14Ru**, indicate improved therapeutic properties when compared to oxaliplatin, the standard CC chemotherapeutic metallo-drug.

2. Results and Discussion

2.1. Synthesis and Characterization

The carbohydrate derivative ligands **L1**-**L4** were prepared from commercially available D-ribose, D-xilose, D-galactose and D-glucose, respectively, in a straightforward one-pot procedure, by reaction of the raw sugars with hydroxylamine hydrochloride in pyridine and *in situ* dehydration of the oximes with acetic anhydride, resulting in the corresponding *O*-acetyl-protected nitrile ligands (Scheme 1). The synthesis of ligands **L5**-**L8** had already been previously reported by some of us[7m] (Scheme 1).

Scheme 1. Synthesis of the carbohydrate derivatives **Lc** and organometallic compounds **1-23** (all with PF_6^- counterion).

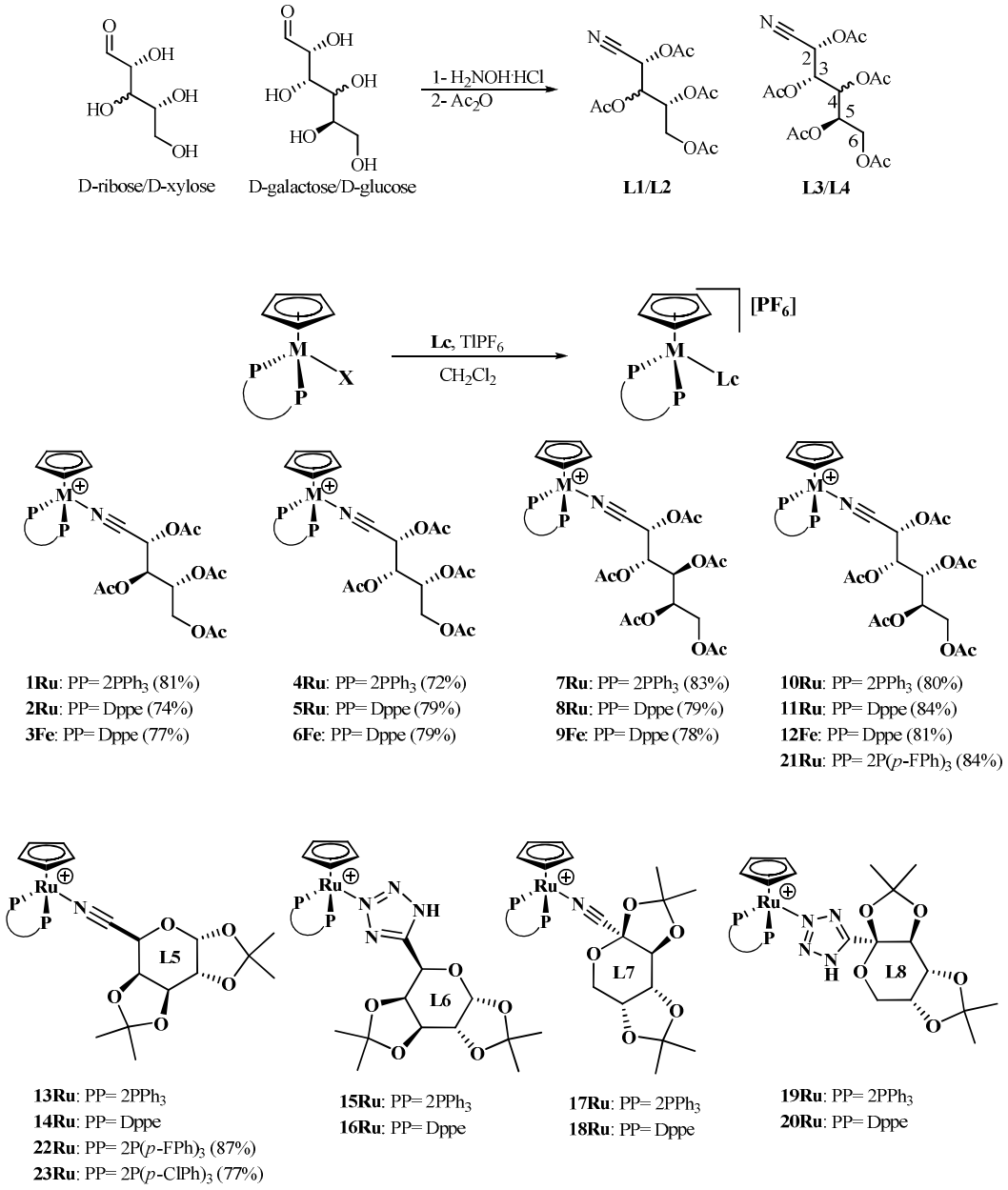

The organometallic compounds of general formula $[(\eta^5\text{-}C_5H_5)M(PP)\mathbf{Lc}][PF_6]$ were prepared by halide abstraction from the parent neutral complexes $[(\eta^5\text{-}C_5H_5)M(PP)X]$ in the presence of a slight excess of the corresponding carbohydrate derivative ligand **Lc**, in dichloromethane at room temperature (Scheme 1). Compounds were recrystallized by slow diffusion of *n*-hexane in dichloromethane solutions.

All new compounds were fully characterized by FT-IR, ^{1}H, ^{13}C, and ^{31}P NMR spectroscopies, and by elemental analysis, corroborating the proposed formulations and structures. The solid state FT-IR spectra of the complexes presents characteristic bands of Cp rings (3055-3075 cm^{-1}), the hexafluorophosphate anion (~ 840 and 560 cm^{-1}) and the coordinated carbohydrate moieties (~ 1750 ($\nu_{C=O}$), ~ 1210 (ν_{C-O})). The $\nu_{C\equiv N}$ band is not visible in the FT-IR spectra of the free ligands, but appears as a medium intensity band at ~ 2250 cm^{-1} for Ru(II) compounds and at ~ 2230 cm^{-1} for Fe(II) analogues. ^{1}H and ^{13}C resonances of the cyclopentadienyl ring are within the characteristic range for monocationic Ru(II) and Fe(II) complexes, at 4.50 – 4.60 ppm for Fe and Ru(P(*p*-YPh)$_3$)$_2$ (Y = H, F, Cl) compounds and at ~ 4.80 ppm for $[(\eta^5\text{-}C_5H_5)Ru(Dppe)]^+$ analogues.[7a,14] In compounds with Dppe as co-ligand, the protons of **Lc** ligands display a general up-field upon coordination; for P(*p*-YPh)$_3$ analogues, chemical shifts remain almost unchanged. Up-field shifts up to 1.2 ppm for H2 of **8Ru** and up to 0.9 ppm for H4 of **5Ru** are attributed to the anisotropic effect of the neighbor phosphine aromatic rings. As discussed for compounds **13Ru-20Ru**,[7m] the aliphatic nature of the ligands excludes the possibility of π-backdonation throughout the carbohydrate backbone.[7a,14] This shielding effect is apparently larger for $[(\eta^5\text{-}C_5H_5)Ru(Dppe)\mathbf{Lc}]^+$ compounds than to their Fe(II) analogues, but a direct comparison cannot be made, since the spectra were determined in different solvents.

^{13}C NMR spectra show the chemical shifts of **Lc** ligands carbon atoms almost un-shifted upon coordination, which further supports the stereochemical nature of the shielding effect verified for the respective protons. Nitrile carbon atoms are the only exception, with low-field shifts upon coordination ranging from ~ 9 ppm for $[(\eta^5\text{-}C_5H_5)Ru(Dppe)\mathbf{Lc}]^+$ compounds, to ~ 16 ppm for the Fe(II) counterparts. Concerning Ru(II) compounds, the nitrile carbon of $[(\eta^5\text{-}C_5H_5)Ru(P(p\text{-}YPh)_3)_2\mathbf{Lc}]^+$derivatives is

more de-shielded upon coordination (~ 13 ppm) than in the Dppe counterparts, consistent with the lower electronic density of the metal center in the $[(\eta^5\text{-}C_5H_5)Ru(p\text{-}YPPh_3)_2\mathbf{Lc}]^+$ moiety.[12] The higher low-field shifts verified for Fe(II) compounds can be explained by the harder metal center and a consequently stronger σ-donation from the nitrile. ^{31}P NMR spectra of the complexes present two doublets, attributed to the phosphine co-ligands, due to a non-equivalence of the coordinated phosphorus atoms, as a result of the asymmetry induced in the metal center by the chiral carbohydrate-derived ligands; one exception is observed for **4Ru** and **22Ru**, which presents an "uncharacteristic" singlet. $^2J_{PP}$ coupling constants of $[(\eta^5\text{-}C_5H_5)Ru(P(p\text{-}YPh)_3)_2\mathbf{Lc}]^+$complexes lie within the range 34.0-36.9 Hz, while for $[(\eta^5\text{-}C_5H_5)Ru(Dppe)\mathbf{Lc}]^+$derivatives it lies within the range 22.5-25.5 Hz. This difference is explained attending the different P-Ru-P angles: $P(p\text{-}YPh)_3$ has larger cone angles, thus leading to a larger P-Ru-P angle and subsequently to a larger $^2J_{PP}$.[15] For the Fe(II) compounds, the $^2J_{PP}$ coupling constants lie within the range 31.4-33.5 Hz, larger than their Ru(II)-Dppe analogues. Fe-P bonds are shorter than Ru-P bonds and P-Fe-P angles are consequently larger than P-Ru-P angles, explaining the larger $^2J_{PP}$ coupling constants verified for Fe analogues. ^{31}P NMR spectra of the complexes also display a septupletat ~ -144 ppm, a characteristic of hexafluorophosphate counter-ion.

Stability of organometallic compounds in stock solution conditions, used in cytotoxic studies, was accessed by ^{31}P NMR spectroscopy. The spectra were determined in DMSO-d_6, following sample preparation and after two weeks of air and moisture exposure, revealing no decomposition within this period. Stability studies in aqueous media were attempted using ^{31}P NMR and UV-Vis spectroscopies, but failed due to extremely low solubility of the compounds in this media.

Suitable crystals for X-ray diffraction studies were obtained by slow diffusion of *n*-hexane in dichloromethane solutions of **3Fe** (Figure 3A), **6Fe** (B), **10Ru** (C), **11Ru** (D) and **12Fe** (E). Compound **3Fe** crystallizes in orthorhombic crystalline system, space group $P2_12_12_1$, and all others in monoclinic system, space group $P2_1$.

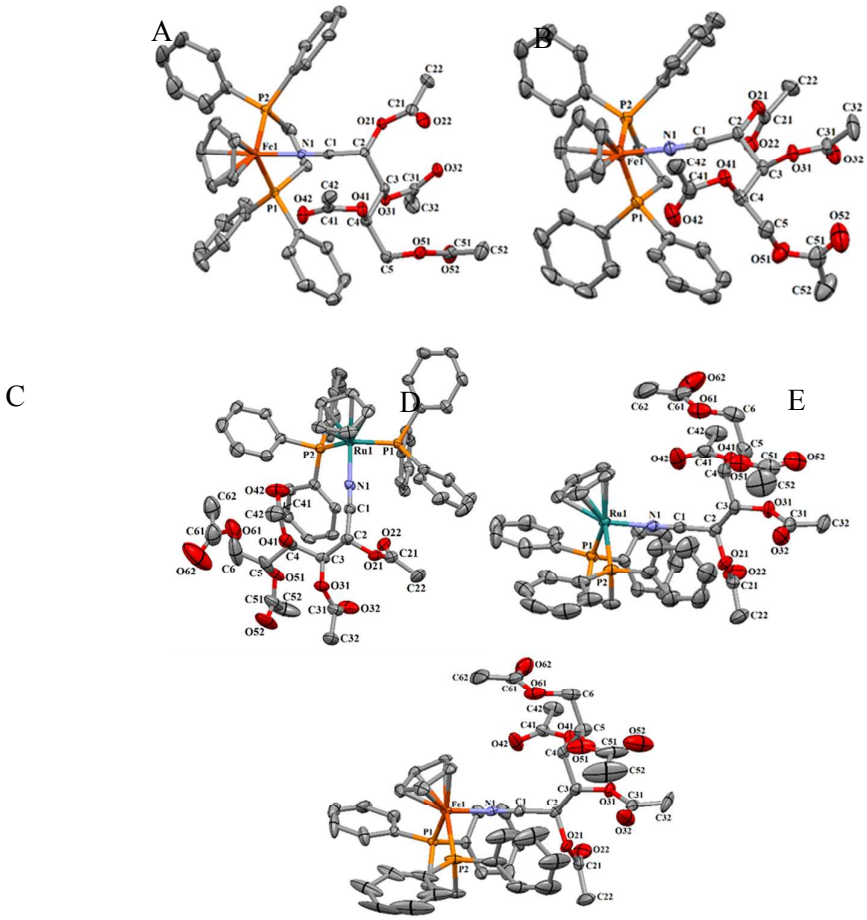

Figure 3. Crystal structure of organometallic cations **3Fe** (A), **6Fe** (B), **10Ru** (C), **11Ru** (D) and **12Fe** (C), with atom labeling. Displacement ellipsoids are drawn at the 50% probability level. Hydrogen atoms are omitted for picture clarity.

Cationic complexes present the usual distorted three-legged piano stool geometry for η^5-monocyclopentadienyl complexes, with $(\eta^5\text{-}C_5H_5)^{Cent}$-M-X angles (X = N, P) ranging from 119.38(17)º to 131.86(14)º, within the range found for analogous compounds.[14] Compound **10Ru** presents a P-Ru-P angle of 98.26(4) whereas for complexes **3Fe**, **6Fe**,

11Ru and **12Fe**, the geometry is restricted by the bite angle of Dppe, with P-M-P angles of 86.31(4), 86.44(6), 83.83(5) and 86.41(5), respectively; the smaller P-Ru-P angle for **11Ru** is rationalized attending to longer Ru-P distances (~ 2.29 Å), in comparison to Fe-P distances (~ 2.21 Å), in perfect agreement with ^{31}P NMR results interpretation (see above).

Although an exhaustive X-ray data discussion falls outside the scope of this article, it is important to notice that, due to the structural similarity of the compounds studied, the differences in cytotoxic activity must be closely linked to the 3D arrangement of the cationic complexes. A structural comparison of the three iron compounds confirms the stereochemistry and chain lengths of the different carbohydrate derivative ligands. The pentose derivative ligands in **3Fe** and **6Fe** adopt the same relative orientation, with the C2-H2 bonds oriented "upwards", roughly towards the (η^5-C_5H_5) ring, confirming the different configurations at C3 stereocenter (Figure 3A and B, respectively). The conformation adopted by the glucose derivative ligand **L4** in compounds **10Ru**, **11Ru** and **12Fe** seems to depend mainly on the stereochemical environment created by the phosphane co-ligands. In compound **10Ru**, the C(2)-C(6) chain extends sideward in relation to Ru-(η^5-C_5H_5) direction, "accommodating" between two Ph rings of the same PPh_3 (Figure 3C). On the other hand, in compounds **11Ru** and **12Fe** (Figure 3D and E, respectively) **L4** extends upwards, minimizing the steric interaction with Ph rings of different P atoms and hindering the metal centers.

2.2. *Cytotoxic studies*

The cytotoxic activity of the organometallic compounds **1-23** was evaluated in HCT116 CC cells. The IC_{50} values determined are presented in Table 1.

When analyzing compounds **1-12**, bearing the linear *O*-acetylated carbohydrate derivative ligands **L1-L4**, the variation of the cytotoxic activity with the organometallic

moiety, within the same ligand, is IC_{50} ($[(\eta^5\text{-}C_5H_5)Ru(PPh_3)_2]^+$) < IC_{50} ($[(\eta^5\text{-}C_5H_5)Ru(Dppe)]^+$) < IC_{50} ($[(\eta^5\text{-}C_5H_5)Fe(Dppe)]^+$), except for the galactose derivative **L3**, in which case the order of Ru(II) moieties is reversed. The best IC_{50} value within this series of compounds was obtained for **10Ru**, bearing the carbohydrate derivative **L4** (IC_{50}= 1.30 μM).

Table 1. IC_{50} values of the organometallic compounds **1-23**, oxaliplatin (positive control) and 5-FU[17] in HCT116 CC cells, after 72h of compound exposure.

Compound	IC_{50} (μM)	95% CI	**Compound**	IC_{50} (μM)	95% CI
1Ru	1.52	1.68-1.81	**13Ru**	1.32	1.22-1.43
2Ru	3.37	3.08-4.03	**14Ru**	0.45	0.44-0.46
3Fe	36.53	30.82-43.30	**15Ru**	1.60	1.52-1.68
4Ru	1.96	1.88-2.05	**16Ru**	6.88	6.54-7.24
5Ru	5.42	5.12-5.84	**17Ru**	1.16	1.10-1.23
6Fe	26.77	21.03-34.07	**18Ru**	0.44	0.43-0.46
7Ru	2.46	2.23-3.25	**19Ru**	1.31	1.24-1.39
8Ru	1.50	1.42-1.59	**20Ru**	3.95	3.79-4.12
9Fe	25.81	20.94-31.81	**21Ru**	4.10	2.70-6.68
10Ru	1.30	1.22-1.38	**22Ru**	3.71	1.67-9.65
11Ru	2.14	1.88-2.44	**23Ru**	9.30	4.38-18.90
12Fe	4.08	3.64-4.58	Oxaliplatin	0.45	0.41-0.48
			5-FU	3.80	

Although $[(\eta^5\text{-}C_5H_5)Fe(Dppe)]^+$ derivatives have recently been studied for their anticancer properties,[11] this is the first time where a direct comparison between iso-structural Ru(II) and Fe(II) compounds can be established. All Fe(II) compounds revealed less cytotoxic against HCT116 cancer cells than their Ru(II)Dppe counterparts. Compounds **3Fe**, **6Fe** and **9Fe**, with ligands **L1-L3** revealed much higher IC_{50} than its Ru(II) analogues, while compound **12Fe**, bearing the glucose derivative **L4**, revealed an IC_{50} of 4.08 μM, only ~ 2x higher than the iso-structural **11Ru**. This value lies within the IC_{50} range spanned by Ru(II) compounds and roughly matches 5-FU IC_{50} (3.80

μM),[16] a current standard in CC chemotherapeutics. As discussed above for X-ray diffraction and NMR spectroscopic data, 3D structural features imposed by the different carbohydrate and organometallic moieties may be at the origin of these differences in cytotoxicity. Moreover, **L3** and **L4,** obtained from galactose and glucose, respectively, differ only in the stereocenter at C4, giving rise to a huge difference in the cytotoxic activity of the corresponding iron complexes **9Fe** (IC_{50} 25.81 μM) and **12Fe** (IC_{50} 4.08 μM), further supporting the importance of stereochemical features for the high cytotoxic activity of **12Fe**.

With regard to compounds **13-20**, the best cytotoxic results were obtained for the $[(\eta^5\text{-}C_5H_5)Ru(Dppe)]^+$ derivatives **14Ru** (IC_{50}= 0.45 μM) and **18Ru** (IC_{50}= 0.44 μM), bearing the galactose and fructose nitrile derivative ligands **L5** and **L7**, respectively, matching the activity of the cornerstone CC metallo-drug oxaliplatin; the corresponding $[(\eta^5\text{-}C_5H_5)Ru(PPh_3)_2]^+$ derivatives **13Ru** and **17Ru**, respectively, revealed it selves less cytotoxic than the Dppe counterparts.

In all cases, organometallic compounds with tetrazole ligands **L6** and **L8** showed less inhibitory effects than the compounds bearing the respective nitrile analogues, but while $[(\eta^5\text{-}C_5H_5)Ru(PPh_3)_2]^+$ derivatives show a minimum difference , for$[(\eta^5\text{-}C_5H_5)Ru(Dppe)]^+$ derivatives, IC_{50}'s varies from 0.45 μM (**14Ru**) to 6.88 μM (**16Ru**) for compounds with **L6**, and slightly less for compounds with **L8**.

So far, Dppe and PPh_3 were the only phosphane co-ligands used in anticancer compounds of general formula $[(\eta^5\text{-}C_5H_5)Ru(PP)(L)][X]$. Compounds **21-23Ru** were synthesized to evaluate the effect of halogenated 4-phenylphosphanes in the cytotoxicity of derivative complexes, when compared to PPh_3. Fluorine is well known to impart special physicochemical and pharmacological properties on drug candidates, being present in 15–20% of currently approved drugs,[17] including anticancer agents (e.g. 5-

Fluorouracil, Fludarabine), and chlorine is also present in chemotherapeutic drugs (e.g. Cladribine). The results were somehow disappointing, since all three compounds revealed it selves less cytotoxic than the PPh_3 analogues. Nonetheless, compounds **21Ru** and **22Ru**, bearing P(*p*-FPh)$_3$ phosphane co-ligands, revealed IC_{50} values within the range spanned by Ru derivatives (4.10 and 3.71 μM, respectively) while compound **23Ru**, the chlorinated analogue of **13Ru** and **22Ru**, was revealed the least cytotoxic of Ru derivatives (IC_{50} = 9.30 μM).

Compounds **14Ru** and **18Ru** revealed the same cytotoxicity against HCT116 CC cells (IC_{50} = 0.45 and 0.44 μM, respectively); for HeLa cancer cells (cervical carcinoma), the galactose derivative **14Ru**(IC_{50} = 3.58 μM) proved more cytotoxic than its fructose analogue **18Ru** (IC_{50} = 6.07 μM)[7m] and less cytotoxic than **13Ru**, bearing PPh_3 co-ligands (IC_{50} = 2.63 μM).

Next, the cytotoxicity mechanisms triggered by compound **8Ru** (IC_{50} = 1.50 μM) and **14Ru** (IC_{50} = 0.45 μM), both $[(\eta^5\text{-}C_5H_5)Ru(Dppe)]^+$ derivatives bearing galactose derivative ligands in open-chain (**L3**) and cyclic (**L5**) forms, respectively, were further explored.

First, cell viability and general cell death were evaluated following HCT116 cell exposure to IC_{50}, 1 and 2 μM of **8Ru**, **14Ru** and oxaliplatin, for 72 h, respectively by ApoToxGlo Triplex Assay, and by lactate dehydrogenase (LDH) release assay. Our results show that for IC_{50} concentrations, and similarly to oxaliplatin, exposure to both **8Ru** and **14Ru** led to significantly reduced cell viability ($p < 0.01$) (Figure 4A) and increased general cell death ($p < 0.01$) (Figure 4B), whereas compared to vehicle control (DMSO). Moreover, in HCT116 cells, exposure to 1 and 2 μM of **14Ru** induced a dose-dependent effect, further decreasing cell viability to 40 and 16 % ($p < 0.01$) (Figure 4A) and enhancing cell death by 1.5- to 2.7-fold ($p < 0.01$) (Figure 4B),

respectively, whereas compared to vehicle control. In turn, no significant increase in the cytotoxic effect of **8Ru** was seen when exposing cells to 1 μM of this compound, while 2 μM exposure induced a modest 25% decrease in cell viability (Figure 4A), and a 1.18-fold increase in in cell death ($p < 0.01$) (Figure 4B).

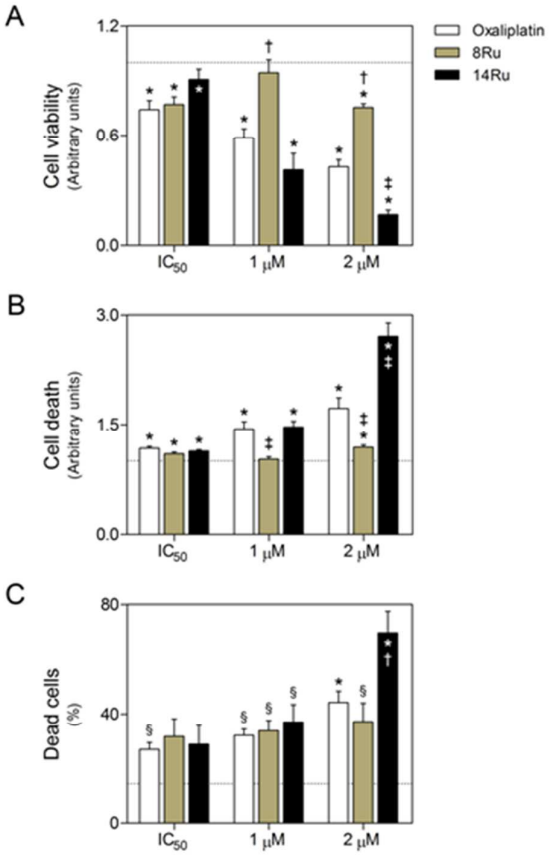

Figure 4. Evaluation of the cytotoxic effects of compounds **8Ru**, **14Ru** and oxaliplatin, on HCT116 human CC cells. Cells were exposed to IC_{50}, 1 and 2 μM **8Ru**, **14Ru** or oxaliplatin for 72 h. DMSO was used as a vehicle control. Cell viability (A), general cell death (B) and percentage of dead cells (C), were evaluated using ApoToxGlo Triplex Assay, LDH release assay and trypan blue exclusion assay, respectively. Results are expressed as (**A**, **B**) mean ± SEM fold-change to vehicle treated cells, or as (**C**) percentage of death cells per sample ± SEM, from at least three independent experiments. Dotted lines represent vehicle control results. § $p < 0.05$ and * $p < 0.01$

from vehicle control treated cells; † $p < 0.05$ and ‡ $p < 0.01$ from oxaliplatin treated cells.

More importantly, exposure to **14Ru** was significantly more cytotoxic than oxaliplatin at 2 μM ($p < 0.01$) (Figure 4A and B), highlighting the antitumor potential of this compound when compared to a current standard of care in CC chemotherapy, which presented a similar IC_{50} value to **14Ru** in HCT116 cells (Table 1). In parallel, the cytotoxic effects of organometallic compounds were validated using the trypan blue exclusion assay after 72 h of exposure to IC_{50}, 1 and 2 μM concentrations of the compounds. Our results confirmed the cytotoxicity of all test compounds, and also the significantly increased cytotoxicity of **14Ru** in HCT116 at 2 μM (68 % dead cells) when compared to oxaliplatin at 2 μM (43 % dead cells) ($p < 0.05$) (Figure 4C).

It is well established that chemotherapeutic agents used against tumor cells act by triggering mechanisms of apoptotic cell death. In this context, activation of caspases has been shown to be a hallmark of drug-induced cellular apoptosis.[18] In addition, apoptotic cell death is characterized by distinctive morphological changes, including cell shrinkage, loss of intercellular membrane contact, progressive condensation of chromatin and cytoplasm, and subsequent nuclear fragmentation. These events culminate in a characteristic formation of apoptotic bodies, consisting of nuclear fragments and intact cell organelles surrounded by a plasma membrane.[19] Therefore, we assessed caspase-3/7 activation using Caspase-Glo 3/7 Assay (Promega), and apoptosis induction by evaluation of nuclear morphology under fluorescent microscopy following staining with the DNA-binding stain Hoechst, upon HCT116 cell exposure to IC_{50}, 1 and 2 μM of **8Ru**, **14Ru** and oxaliplatin for 24 h and 72 h, respectively. Our data showed that similarly to oxaliplatin, both **8Ru** and **14Ru** triggered apoptotic cell death,

leading to a significant increase in caspase-3 and -7 activity ($p < 0.05$) (Figure 5A) and apoptotic cells ($p < 0.01$) (Figure 5B and C), whereas compared to vehicle control cells. Moreover, our results established that **14Ru** induced a 1.4-fold increase in caspase-3 and -7 activity at IC_{50}, which was significantly higher than oxaliplatin's ($p < 0.05$), which increased caspase-3 and -7 activity only by 1.27-fold ($p < 0.01$) (Figure 5A). Hereupon, **14Ru** exposure induced a dose-dependent increase in HCT116 apoptosis, leading to up to 16 , 22 and 43 % of apoptotic cells at IC_{50}, 1 and 2 μM, respectively, whereas compared to vehicle control exposure ($p < 0.01$) (Figure 5B). In contrast, exposure to 2 μM **8Ru** led to less than 25 % of apoptotic events ($p < 0.01$) (Figure 5B). It should be emphasized that **14Ru** also induced significantly higher levels of apoptosis than oxaliplatin at 2 μM ($p < 0.01$), which was shown to trigger apoptosis in 30 % of HCT116 cells ($p < 0.01$) (Figure 5B).

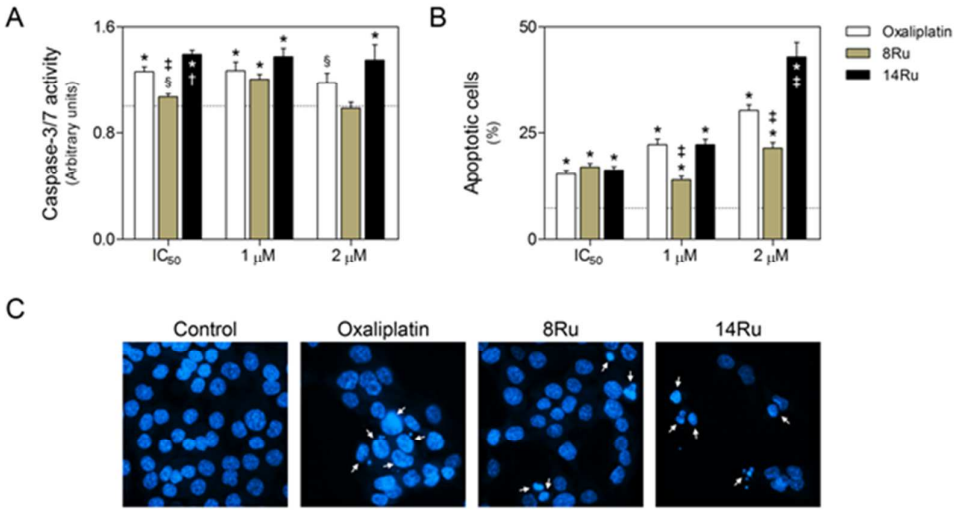

Figure 5. Evaluation of the apoptotic effects of compounds **8Ru**, **14Ru** and oxaliplatin on HCT116 human CC cells. Cells were exposed to IC_{50}, 1 and 2 μM of **8Ru**, **14Ru** or oxaliplatin. DMSO was used as a vehicle control. (A) Caspase-3/7 activity was determined at 24 h of compound exposure using the Caspase-Glo 3/7 Assay. (B) Nuclear morphology after Hoechst staining was evaluated by fluorescence microscopy

at 72 h of compound exposure. Dotted lines represent vehicle control results. (C) Representative images of Hoechst staining at 400x magnification. Arrows indicate nuclear fragmentation and chromatin condensation. Results are expressed as (**A**) mean ± SEM fold-change to vehicle treated cells, or as (**B**) percentage of apoptotic cells per field ± SEM, from at least three independent experiments. § $p < 0.05$ and * $p < 0.01$ from vehicle control treated cells; † $p < 0.05$ and ‡ $p < 0.01$ from oxaliplatin treated cells.

Collectively, our data indicate that **8Ru** and **14Ru** are capable of markedly decreasing cell viability and inducing apoptotic cell death in HCT116 human CC cells. More importantly, **14Ru** was shown to trigger significantly higher levels of apoptosis when compared to oxaliplatin, the cornerstone colon cancer chemotherapeutic agent.

3. Experimental Section

All experiments were carried out under inert atmosphere (N_2) using standard Schlenk techniques. Commercial reagents were bought from Sigma-Aldrich and used without further purification. All solvents were dried using standard methods.[20] Starting materials were prepared following the methods described in the literature for the synthesis of [(η^5-C_5H_5)Ru(Dppe)Cl], [(η^5-C_5H_5)Ru(PPh_3)$_2$Cl][21] and [(η^5-C_5H_5)Fe(Dppe)I].[22] Compounds [(η^5-C_5H_5)Ru(P(*p*-FPh)$_3$)$_2$Cl] and [(η^5-C_5H_5)Ru(P(*p*-ClPh)$_3$)$_2$Cl] are here first described, and were synthesized adopting the procedure used for the synthesis of [(η^5-C_5H_5) Ru(PPh_3)$_2$Cl], as described below. Solid state IR spectra were recorded in a Jasco FTIR-4100 spectrophotometer with KBr pellets; only significant bands were cited in the text. ^{1}H, ^{13}C and ^{31}P NMR spectra were recorded on Bruker Avance II 400 or Bruker Avance II 300 spectrometers, at probe temperature. The ^{1}H and ^{13}C NMR chemical shifts are

reported in parts per million (ppm) downfield from the residual solvent peak; ^{31}P NMR spectra are reported in ppm downfield from external standard H_3PO_4 85%. Coupling constants are reported in Hz. Assignments of ^{1}H and ^{13}C NMR spectra were confirmed with the aid of two dimensional techniques ^{1}H, ^{13}C (COSY, HSQC). Microanalyses were performed at Laboratório de Análises do Instituto Superior Técnico, using a Fisons Instruments EA1108 system and data acquisition, integration and handling were performed using the software package Eager-200 (Carlo Erba Instruments), confirming ≥ 95% purity for all the tested compounds.

General procedure for the synthesis of ligands ***Lc***: To a solution of carbohydrate (10 mmol) in pyridine (5 mL) was added $H_2NOH{\cdot}HCl$ (12 mmol) and the mixture was stirred for 2h. Ac_2O was then added (5 mL) and the mixture stirred at r.t. for further 2h. The solvent was then removed and the crude was extracted with AcOEt (3 x 20 mL), filtered and pumped to dryness. The crude obtained was purified by column chromatography (AcOEt:*n*-hexane), affording the pure *O*-acetylated nitrile ligands as a white crystalline solids.

General procedure for the synthesis of complexes $[(\eta^5\text{-}C_5H_5)Ru(P(p\text{-}YPh)_3)_2Cl]$ *(Y = F, Cl)*: To a boiling solution of $RuCl_3{\cdot}xH_2O$ (1.0 g) and freshly distilled cyclopentadiene (5 mL) in ethanol (80 mL), was added $P(p\text{-}YPh)_3$ (12 mmol) and the mixture was stirred for 2h. After cooling to r.t., the solvent was removed by filtration and the solid products were washed with ethanol (3 x 20 mL) and *n*-hexane (3 x 20 mL). The products were recrystallized from dichloromethane solutions, by addition of *n*-hexane, affording crystalline compounds.

General procedure for the synthesis of complexes $[(\eta^5\text{-}C_5H_5)M(P\text{–}P)(\mathbf{Lc})][PF_6]$: To a schlenck charged with $[(\eta^5\text{-}C_5H_5)M(P\text{–}P)X]$ (0.20 mmol), $TlPF_6$ (0.20 mmol) and **Lc** (0.22 mmol) was added dichloromethane (20 mL), and the mixture was stirred

overnight at room temperature, under inert atmosphere. The solutions were double filtered and pumped to dryness, and the crude compounds were then washed with *n*-hexane and recrystallized by slow diffusion of *n*-hexane in dichloromethane solutions, affording crystalline products.

X-ray Diffraction Studies. Suitable crystals for X-ray diffraction studies were obtained by slow diffusion of hexane into dichloromethane solutions of **3Fe**, **6Fe**, **10Ru**, **11Ru** and **12Fe**. Data were collected at 150 K using a Bruker AXS-KAPPA APEX II diffractometer. Structure resolution was performed with SHELXS97 and refinement with SHELXL97. H atoms were calculated and constrained as riding on their bound atoms. CCDC 1050669 to 1050673 contains the supplementary crystallographic data for this paper (**3Fe**, **6Fe**, **10Ru**, **11Ru** and **12Fe**, respectively). These data can be obtained free of charge via www.ccdc.cam.ac.uk/data_request/cif or by emailing data_request@ccdc.cam.ac.uk or by contacting The Cambridge Crystallographic Data Centre, 12, Union Road, Cambridge CB2 1EZ, UK; fax +44 1223 336033.

Cell culture. HCT116 human colon carcinoma cells were grown in McCoy's 5A modified medium supplemented with 10% heat-inactivated fetal bovine serum (FBS) and 1 % antibiotic/antimycotic solution (Gibco, Life Technologies, Paisley, UK), and cultured at 37 °C under a humidified atmosphere of 5 % CO_2. Cells were seeded in 96-well plates at 1 x 10^4 cells/well for dose-response curves, cell viability and cell death assays; and at 1.5 x 10^4 cells/well for caspase activity studies. Additionally, cells were seeded in 24-well plates at 5x10^4 cells/well for trypan blue exclusion assay, and in 35 mm dishes at 3 x 10^5 cells/dish for morphological assessment of apoptosis.

Exposure to organometallic compounds. Stock solutions of the organometallic complexes **1-23** were prepared in sterile DMSO. Prior to all treatments, the cells were allowed to adhere for 24 h, and then exposed to test compounds for the mentioned time.

To plot dose-response curves, cells were exposed to 0.1–100 μM test compounds for 72 h. For cell viability, cell death and apoptosis studies, metal-based compounds were tested at IC_{50}, 1 and 2 μM, for 24 to 72 h. All experiments were performed in parallel with DMSO vehicle control. Oxaliplatin, a cytotoxic agent used in colon cancer treatment, was used as a positive control in all assays. The final DMSO concentration was always of 0.1 %.

Dose-response curves. To plot dose-response curves, cell viability was evaluated using the CellTiter 96 AQ_{ueous} Non-Radioactive Cell Proliferation Assay (Promega, Madison, WI, USA), according to the manufacturer's instructions. This colorimetric assay is based on the bio-reduction of 3-(4,5-dimethylthiazo-2-yl)-5-(3-carboxymethoxyphenyl)-2-(4-sulfophenyl)-2H-tetrazolium inner salt (MTS) to formazan by dehydrogenase enzymes found within metabolically active cells. The amount of water soluble formazan product can be measured by the amount of 490 nm absorbance, correlating with the number of living cells in culture. For this purpose, changes in absorbance were assessed using a Model 680 microplate reader (Bio-Rad, Hercules, CA, USA). Best-fit IC_{50} values from at least three independent experiments were calculated using GraphPad Prism software (version 5.00; San Diego, CA, USA), using the log (inhibitor) *vs* response (variable slope) function.

Evaluation of cell viability. Cell viability was evaluated using the ApoToxGlo Triplex Assay (Promega), according to the manufacturer's instructions. This assay uses a fluorogenic, cell-permeant, peptide substrate (glycylphenylalanyl-aminofluorocoumarin; GF-AFC) that may be cleaved by a protease found exclusively within intact cells to release AFC, generating a fluorescent signal proportional to the number of living cells. In brief, 20 μL of GF-AFC substrate solution was added to each well, and plates were incubated at 37 °C for 1 h. Fluorescence emission was detected using a GloMax-Multi+

Detection System (Promega), with an at 405 nm excitation filter and at 495-505 nm emission filter.

Evaluation of cell death. General cell death was evaluated using the Cytotoxicity Detection Kit^{PLUS} (Roche Diagnostics GmbH, Mannheim, Germany) to measure the amount of cytoplasmic lactate dehydrogenase (LDH) released from plasma membrane-damaged cells into the extracellular medium. Thereby, the amount of enzyme activity on supernatants can be proportionally determined by a coupled enzymatic reaction whereby the *p*-iodonitrotetrazolium salt is reduced to a red formazan product that can be spectrophotometrically quantified at 490 nm. For the LDH assay, 50 µL of culture supernatant was collected from each well into a new 96-well plate to evaluate LDH release. In parallel, the remaining cells attached to the original plate were lysed in 50 µL of medium to release the intracellular LDH. Subsequently, supernatant samples and total cell lysates were incubated with 50 µL of assay substrate for 10 to 30 min, at room temperature, protected from light. Absorbance readings were measured spectrophotometrically at 490 nm, with a 620 nm reference wavelength, using a Model 680 microplate reader (Bio-Rad). The percentage of LDH release was determined as the ratio between the released LDH (supernatant) and the total LDH (supernatant + cell lysate).

Additionally, cell death was evaluated using the trypan blue dye exclusion test. This method relies on the principle that live cells retain intact cytoplasmic membranes that exclude trypan blue, remaining unstained, while dead cells incorporate this vital dye into the cytoplasm due to loss of membrane selectivity. To evaluate trypan blue dye intake upon loss of membrane integrity, cell culture supernatants and attached cells were harvested to the same tube, and next collected by centrifugation at 500 *g* for 5 min. Next, supernatants were discarded, and cells were re-suspended and stained in 0.1 %

trypan blue solution diluted in phosphate-buffered saline (PBS). Subsequently, the relative number of dead and live cells was obtained by optical microscopy by counting the number of blue-stained (dead) and unstained (live) cells using a Neubauer chamber.

Evaluation of apoptotic cell death. Activity of effector caspase-3 and -7 was measured using the Caspase-Glo 3/7 Assay (Promega). This assay is based on the cleavage of a pro-luminescent substrate containing the specific DEVD sequence recognized by caspase-3 and -7 to release aminoluciferin in cell lysates. The subsequent luciferase cleavage of the unconjugated aminoluciferin generates a luminescent signal directly proportional to the amount of caspase activity present in the sample. For this purpose, 75 µL of Caspase-Glo 3/7 reagent was added to each well, and the mixture was incubated at room temperature for 30 min, leading to complete cell lyses, stabilization of substrate cleavage by caspases, and accumulation of luminescent signal. The resulting luminescence was measured using the GloMax-Multi+ Detection System (Promega).

Nuclear morphology was assessed using the DNA-binding stain Hoechst to identify apoptotic cells based on their typical morphological changes. In brief, attached cells were fixed with 4 % paraformaldehyde in PBS for 20 min, stained with 5 mg/mL Hoechst 33258 dye (Sigma Aldrich, St. Louis, MO, USA) in PBS for 15 min, washed with PBS, and mounted with cover slips using PBS/glycerol (3:1). Nuclear morphology was evaluated by fluorescence microscopy, under 400x magnification, and nuclei were scored and categorized according to condensation and staining characteristics of chromatin. Normal nuclei showed non-condensed chromatin dispersed over the entire nucleus. Apoptotic nuclei were identified by condensed chromatin, contiguous to the nuclear membrane, as well as nuclear fragmentation. A minimum of five random

microscopic fields with approximately 100 nuclei were counted for each condition and the results were expressed as the percentage of apoptotic nuclei per field.

Statistical Analysis. All data were expressed as mean ± standard error of mean (SEM) from at least three independent experiments. Statistical analysis was performed using Student's *t*-test. Values of $p < 0.05$ were considered significant.

4. Conclusions

This study provides a first insight on cyclopentadienyl-ruthenium(II) and iron(II) complexes with bio-derivative moieties as CC chemotherapeutic agents. The ligands **Lc** are obtained from inexpensive raw carbohydrates using simple synthetic procedures, and taking advantage of both cyclic and open chain forms of these biomolecules. The cytotoxic activity of twenty three organometallic compounds of general formula [(η^5-C_5H_5)M(PP)**Lc**][PF_6] was evaluated in HCT116 CC cells, with two ruthenium compounds, **14Ru** and **18Ru**, matching the IC_{50} of oxaliplatin, and compound **12Fe** revealing high cytotoxicity, roughly matching the IC_{50} of 5-FU, the non-metallic CC chemotherapeutic cornerstone. SAR's data analysis shows a dependency of the cytotoxic activity on the carbohydrate moiety (sugar and open-chain/cyclic form), linker (nitrile, tetrazole), metal (Ru, Fe) and co-ligands (Dppe, PPh_3, P(*p*-FPh)$_3$, P(*p*-ClPh)$_3$). Our leading compound, **14Ru**, showed improved cytotoxic properties, when compared to oxaliplatin, the cornerstone chemotherapeutic metallo-drug used in CC treatment. This compound induces dose-dependent HCT116 general cell death, triggering higher levels of caspase-3 and -7 activities, and apoptosis in a dose dependent manner. Taken together, these results highlight the potential of ruthenium and iron organometallic compounds bearing carbohydrate moieties as rising opportunities to develop alternative anticancer drugs, with very high potential for surpassing problems

such as general toxicity, side effects and drug resistance, the current major obstacles in colon cancer treatment.

ASSOCIATED CONTENT

Supporting Information. Full spectroscopic characterization by FT-IR, ^{1}H-, ^{13}C-, ^{31}P NMR (spectra description and interpretation) and elemental analysis of compounds **L1**-**L4**, [(η^5-C_5H_5)Ru(P(*p*-FPh)$_3$)$_2$Cl], [(η^5-C_5H_5)Ru(P(*p*-ClPh)$_3$)$_2$Cl] and compounds **1**-**23**, and further X-ray experimental details. This material is available free of charge via the Internet at http://pubs.acs.org.

AUTHOR INFORMATION

Corresponding Author

* PRF email: pedro.florindo@tecnico.ulisboa.pt

* ACF email: anacristinafernandes@tecnico.ulisboa.pt

ACKNOWLEDGMENT

This research was supported by FCT through projects PTDC/QUI-QUI/102114/2008 and PTDC/QUI-QUI/110532/2009 and annual funds UID/QUI/00100/2013. PRF and DMP (SFRH/BD/96517/2013) thank FCT for grants. Authors thank the Portuguese NMR Network (IST-UTL Center) for providing access to the NMR facilities..

REFERENCES

(1) (a) Rosenberg, B.; Van Camp, L.; Krigas, T. Inhibition of cell division in Escherihia Coli by electrolysis products from a platinum electrode. *Nature* **1965**, 205, 698–699. (b) Rosenberg, B.; Vancamp, L.; Trosko, J. E.; Mansour V. H. Platinum Compounds: a New Class of Potent Antitumor Agents. *Nature* **1969**, 222, 385–386.

(2) (a)Yan, Y. K.; Melchart, M.; Habtemariam, A.; Sadler, P. J. Organometallic chemistry, biology and medicine: ruthenium arene anticancer complexes. *Chem.*

Commun. **2005**, 4764-4776. (b) Süss-Fink, G. Arene ruthenium complexes as anticancer agents. *Dalton Trans.* **2010**, 39, 1673-1688. (c) Singha, A.K.; Pandeyb, D.S.; Xua, Q.; Braunstein, P. Recent advances in supramolecular and biological aspects of arene-ruthenium(II) complexes. *Coord. Chem. Rev.* **2014**, 270–271, 31–56. (d) Bergamo, A.; Gaiddon, C.; Schellens, J.H.M.; Beijnen, J.H.; Sava G. Approaching tumour therapy beyond platinum drugs. Status of the art and perspectives of ruthenium drug candidates. *J. Inorg. Biochem.* **2012**, 106, 90-99.

(3) (a) Groessl, M.; Reisner, E.; Hartinger, C.G.; Eichinger, R.; Semenova, O.; Timerbaev, A.R.; Jakupec, M.A.; Arion, V.B.; Keppler, B.K. Structure-activity relationships for NAMI-A-type complexes (HL)[trans-$RuCl_4$L(S-dmso)ruthenate(III)] (L = imidazole, indazole, 1,2,4-triazole, 4-amino-1,2,4-triazole, and 1-methyl-1,2,4-triazole): aquation, redox properties, protein binding, and antiproliferative activity. *J. Med. Chem.* **2007**, 50, 2185–2193.

(4) Hartinger, C.G.; Zorbas-Seifried, S.; Jakupec, M.A.; Kynast, B.; Zorbas, H.; Keppler, B. K. From bench to bedside-preclinical and early clinical development of the anticancer agent indazolium trans-[tetrachlorobis(1H-indazole)ruthenate(III)] (KP1019 or FFC14A). *J. Inorg. Biochem.* **2006**, 100, 891–904.

(5) Rademaker-Lakhai, J.M.; van den Bongard, D.; Pluim, D.; Beijnen, J.H.; Schellens, J.H. A phase I and pharmacological study with imidazolium-trans- DMSO-imidazole-tetrachlororuthenate, *Clin. Cancer Res.* **2004**, 10, 3717-3727.

(6) Lentz, F.; Drescher, A.; Lindauer, A.; Henke, M.; Hilger, R.A.; Hartinger, C.G.; Scheulen, M.E.; Dittrich, C.; Keppler, B.K.; Jaehde, U. Pharmacokinetics of a novel anticancer ruthenium complex (KP1019, FFC14A) in a phase I dose-escalation study. *Anticancer Drugs* **2009**, 20, 97-103.

(7) (a) Bregman, H.; Williams, D.S.; Atilla, G.E.; Carroll, P.J.; Meggers, E. An Organometallic Inhibitor for Glycogen Synthase Kinase 3 *J. Am. Chem. Soc.* 2004, 126, 13594-13595. (b) Debreczeni, J.E.; Bullock, A.N.; Atilla, G.E.; Williams, D.S.; Bregman, H.; Knapp, S.; Meggers, E. Extremely Tight Binding of Ruthenium Complex to Glycogen Synthase Kinase 3. *Angewandte Chemie (Int. Ed. in English)* **2006**, 45, 1580-1585. (c) Smalley, K.S.; Contractor, R.; Haass, N.K.; Kulp, A.N.; Atilla-Gokcuman, G.E.; Williams, D.E.; Bregman, H.; Flaherty, K.T.; Soengas, M.S.; Meggers, E.; Herlyn, M. An Organometallic Protein Kinase Inhibitor Pharmacologically Activates p53 and Induces Apoptosis in Human Melanoma Cells. *Cancer Research* **2007**, 67, 209-217. (d) Anand, R.; Maksimoska, J.; Pagano, N.; Wong, E.Y.; Gimotty, P.A.; Diamond, S.L.; Meggers, E.; Marmorstein, R. Toward the Development of a Potent and Selective Organoruthenium Mammalian Sterile 20 Kinase Inhibitor. *J. Med. Chem.* **2009**, 52, 1602-1611. (e) Garcia, M.H.; Morais, T.S.; Florindo, P.; Piedade, M.F.M.; Moreno, V.; Ciudad, C.; Noe, V. Inhibition of cancer cell growth by ruthenium(II) cyclopentadienyl derivative complexes with heteroaromatic ligands. *J. Inorg. Biochem.* **2009**, 103, 354-361. (f) Moreno, V.; Lorenzo, J.; Aviles, F.X.; Garcia, M.H.; Ribeiro, J.; Morais, T.S.; Florindo, P.; Robalo, M.P. Studies of the Antiproliferative Activity of Ruthenium (II) Cyclopentadienyl-Derived Complexes with Nitrogen Coordinated Ligands. *Bioinorg. Chem. App.* **2010**, ID 936834, 1-11. (g) Moreno, V.; Font-Bardia, M.; Calvet, T.; Lorenzo, J.; Avilés, F.X.; Garcia, M.H.; Morais, T.S.; Valente, A.; Robalo, M.P. DNA interaction and cytotoxicity studies of new ruthenium(II) cyclopentadienyl derivative complexes containing heteroaromatic ligands. *J. Inorg. Biochem.* **2011**, 105, 241-249. (h) Tomaz, A.I.; Jakusch, T.; Morais, T.S.; Marques, F.; Almeida, R.F.M.; Mendes, F.; Enyedy, E.A.; Santos, I.; Pessoa, J.C.; Kiss, T.; Garcia, M.H. $[Ru^{II}(\eta^5\text{-}C_5H_5)(bipy)(PPh_3)]^+$, a promising large spectrum antitumor

agent: Cytotoxic activity and interaction with human serum albumin. *J. Inorg. Biochem.* **2012**, 117, 261-269. (i) Morais, T.S.; Santos, F.; Côrte-Real, L.; Marques, F.; Robalo, M.P.; Madeira, P.J.A.; Garcia, M.H. Biological activity and cellular uptake of [Ru(η^5-C_5H_5)(PPh_3)(Me_2bpy)][CF_3SO_3] complex. *J. Inorg. Biochem.* **2013**, 122, 8-17. (j) Valente, A.; Garcia, M.H.; Marques, F.; Miao, Y.; Rousseau, C.; Zinck, P. First polymer "ruthenium-cyclopentadienyl" complex as potential anticancer agent. *J. Inorg. Biochem.* **2013**, 127, 79-81. (k) Morais, T.S.; Santos, F.C.; Jorge, T.F.; Côrte-Real, L.; Madeira, P.J.A.; Marques, F.; Robalo, M.P.; Matos, A.; Santos, I.; Garcia, M.H. New water-soluble ruthenium(II) cytotoxic complex: Biological activity and cellular distribution. *J. Inorg. Biochem.* **2014**, 130, 1-14. (l) Côrte-Real, L.; Mendes, F.; Coimbra J.; Morais, T.S.; Tomaz, A.I.; Valente, A.; Garcia, M.H.; Santos, I.; Bicho, M.; Marques, F. Anticancer activity of structurally related ruthenium(II) cyclopentadienyl complexes. *J. Biol. Inorg. Chem.* **2014**, 19, 853-867. (m) Florindo, P.R.; Marques, I.J.; Nunes, C.D.; Fernandes, A.C. Synthesis, characterization and cytotoxicity of cyclopentadienyl ruthenium(II) complexes containing carbohydrate-derived ligands. *J. Organomet. Chem.* **2014**, 760, 240-247.

(8) (a) Vessieres, A.; Top, S.; Beck, W.; Hillard, E.; Jaouen, G. Metal complex SERMs (selective oestrogen receptor modulators). The influence of different metal units on breast cancer cell antiproliferative effects. *Dalton Trans.* **2006**, 529-541. (b) Top, S.; Vessieres, A.; Leclercq, G.; Quivy, J.; Tang, J.; Vaissermann, J.; Huche, M.; Jaouen, G. Synthesis, biochemical properties and molecular modelling studies of organometallic specific estrogen receptor modulators (SERMs), the ferrocifens and hydroxyferrocifens: evidence for an antiproliferative effect of hydroxyferrocifens on both hormone-dependent and hormone-independent breast cancer cell lines. *Chem. Eur. J.* **2003**, 9, 5223-5236.

(9) Braga, S.S.; Silva, A.M.S. A New Age for Iron: AntitumoralFerrocenes. *Organometallics* **2013**, 32, 5626−5639.

(10) Gasser, G.; Ott, I.; Metzler-Nolte, N. Organometallic Anticancer Compounds. *J. Med. Chem.* **2011**, 54, 3-25.

(11) (a) Gonçalves, A.C.; Morais, T.S.; Robalo, M.P.; Marques, F.; Avecilla, F.; Matos, C.P.; Santos, I.; Tomaz, A.I.; Garcia, M.H. Important cytotoxicity of novel iron(II) cyclopentadienyl complexes with imidazole based ligands. *J. Inorg. Biochem.* **2013**, 129, 1-8. (b) Valente, A.; Santos, A.M.; Côrte-Real, L.; Robalo, M.P.; Moreno, V.; Font-Bardia, M.; Calvet, T.; Lorenzo, J.; Garcia, M.H. New iron(II) cyclopentadienyl derivative complexes: Synthesis and antitumor activity against human leukemia cancer cells.

(13) (a) Mader, R.M.; Muller, M.; Steger, G.G. Resistance to 5-Fluorouracil. *Gen. Pharmac.* **1998**, 31, 661-666; b) Alcindor, T.; Beauger, N. Oxaliplatin: a review in the era of molecularly targeted therapy. *Curr. Oncol.* **2011**, 18, 18-25.

(14) (a) Garcia, M.H.; Florindo, P.; Piedade, M.F.M.; Maiorana, S.; Licandro, E. New organometallic Ru(II) and Fe(II) complexes with tetrathia-[7]-helicene derivative ligands. *Polyhedron* **2009**, 28, 621-629. (b) Garcia, M.H.; Florindo, P.; Piedade, M.F.M.; Duarte, M.T.; Robalo, M.P.; Goovaerts, E.; Wenseleers, W. Synthesis and structural characterization of ruthenium(II) and iron(II) complexes containing 1,2-di-(2-thienyl)-ethene derived ligands as chromophores. *J. Organomet. Chem.* **2009**, 694, 433-445.

(15) Kühl, O. Phosphorous-31 NMR Spectroscopy: A Concise Introduction for the Synthetic Organic and Organometallic Chemist. Springer-Verlag, Berlin, Germany, **2008**.

(16) Mansoor, T.A; Borralho, P.M.; Luo, X.; Mulhovo, S.; Rodrigues, C.M.P.; Ferreira M.-J.U. Acetonyldihydrochelerythrineis a potent inducer of apoptosis in HCT116 and SW620 Colon Cancer cells. *J. Nat. Prod.* **2014**, 77, 1825-1830.

(17) Shah, P.; Westwell A.D. The role of fluorine in medicinal chemistry. *J. Enzyme Inhib. Med. Chem.* **2007**, 22, 527-40.

(18) Kaufmann, S.H.; Earnshaw W.C. Induction of Apoptosis by Cancer Chemotherapy. *Exp. Cell Res.* **2000**, 256, 42-49.

(19) Galluzzi, L.; Aaronson, S.A. *et al.* Guidelines for the use and interpretation of assays for monitoring cell death in higher eukaryotes. *Cell Death Differ.* **2009**, 16, 1093-1107

(20) Perrin, D.D.; Amarego, W.L.F.; Perrin, D.R., *Purification of Laboratory Chemicals*, 2nd ed., Pergamon, New York, **1980**.

(21) Ashby, G.S.; Bruce, M.I.; Tomkins, I.B.; Walli, R.C. Cyclopentadienyl-ruthenium and -osmium Chemistry. VII. Complexes Containing Nitriles, Tertiary Phosphines or Phosphites Formed by Addition or Displacement Reactions. *Aust. J. Chem.* **1979**, 32, 1003-1008.

(22) Garcia, M.H.; Robalo, M.P.; Dias, A.R.; Piedade, M.F.M.; Galvão, A.; Wenseleers, W.; Goovaerts, E. Organometallic complexes for second-order non-linear optics: synthesis and molecular quadratic hyperpolarizabilities of η^5-monocyclopentadienyliron(II) nitrile derivatives with different phosphines. X-ray crystal structure of $[FeCp(Dppe)(p\text{-}NCC_6H_4NO_2)][PF_6]\cdot CH_2Cl_2$. *J. Organomet. Chem.* **2001**, 619, 252-264.

Table of Contents Graphic